

Supporting Information

Nanoporous, Bicontinuous Cubic Lyotropic Liquid Crystal Networks via Polymerizable Gemini Ammonium Surfactants

Evan S. Hatakeyama,[‡] Brian R. Wiesenauer,[‡] Christopher J. Gabriel,[‡] Richard D. Noble,[‡] and Douglas L. Gin^{‡,§*}

[‡]*Department of Chemical & Biological Engineering, and* [§]*Department of Chemistry & Biochemistry, University of Colorado, Boulder, CO 80309*

Materials and General Procedures. Chromium (IV) oxide, pyridine, 9-bromo-1-nonanol, allyltrimethylsilane, *sec*-butyl lithium (1.4 M in cyclohexane), aluminum oxide (activated, basic), 2-isopropoxy-4,4,5,5-tetramethyl-1,3,2-dioxaborolane, *N,N,N',N'*-tetramethylethylene-1,2-diamine, *N,N,N',N'*-tetramethylpropane-1,3-diamine, *N,N,N',N'*-tetramethylhexane-1,6-diamine, and 2-hydroxy-2-methylpropiophenone were obtained from Sigma-Aldrich Co. and used as purchased. 7-Bromo-1-heptanol was purchased from TCI America and used as received. 11-Bromo-1-undecanol was obtained from Fluka and used as purchased. All solvents were purchased from Sigma-Aldrich or Fisher Scientific, and purified/dehydrated via N₂-pressurized activated alumina columns, unless otherwise noted. All chemical syntheses were carried out under a dry argon atmosphere using standard Schlenk line techniques, unless otherwise noted. Filtration through silica gel was performed using 230–400 mesh, normal-phase silica gel purchased from Sorbent Technologies. The water used in LLC phase formulation and water filtration experiments was de-ionized, and had a resistivity of >12 MΩ cm⁻¹. Solupor E075-9H01A microporous support membrane (made from hydrophilically treated, ultrahigh-molecular-weight polyethylene (PE) fiber matte) was provided by DSM Solutech (Geleen, The Netherlands). Mylar sheets were purchased from American Micro Industry, Inc.

Instrumentation. ¹H NMR spectra were obtained using a Bruker 300 Ultrashield™ (300 MHz) spectrometer, Varian Inova 500 (500 MHz), or Inova 400 (400 MHz) spectrometers. Chemical shifts are reported in ppm relative to deuterated solvent. Fourier-transform infrared spectroscopy (FT-IR) measurements were performed using a Matteson Satellite series spectrometer, as thin films on Ge crystals. HRMS analysis was performed by the Central Analytical Facility in the Dept. of Chemistry and Biochemistry at the University of Colorado, Boulder. LLC mixtures were homogenized using an IEC Centra-CL2 centrifuge. Powder X-ray diffraction (XRD) spectra were obtained with an Inel CPS 120 diffraction system using a monochromated Cu K_α radiation source. The apparatus was equipped with a film holder and temperature-programmable heating stage to analyze samples. All powder XRD spectra were calibrated against a silver behenate diffraction standard ($d_{100} = 58.4 \pm 0.1 \text{ \AA}$).¹ Powder XRD measurements were all performed at ambient temperature (21 ± 1 °C). Variable temperature polarized light microscopy (PLM) studies were performed using a Leica DMRXP polarizing light microscope equipped with a Q-Imaging MicroPublisher 3.3 RTV digital camera, a Linkam LTS 350 thermal stage, and a Linkam CI 94 temperature controller. Automatic temperature

profiles and image captures were performed using Linkam Linksys32 software. Images were captured at 125x magnification. Photopolymerizations were conducted using a Spectroline XX-15A 365 nm UV lamp (8.5 mW cm⁻² at the sample surface). UV light fluxes at the sample surface were measured using a Spectroline DCR-100X digital radiometer equipped with a DIX-365 UV-A sensor. Photopolymerizations were conducted on a custom-made temperature-controlled hot stage. Filtration studies were performed using custom designed, stainless steel, stirred, dead-end filtration cells that can accommodate 2.5 cm diameter membrane test samples. The ion conductivity of permeate solutions was measured using a VWR International electrical conductivity meter model 2052-B. Total organic carbon (TOC) analysis of permeate solutions containing organic solutes was conducted using a Test N Tube TOC kit (Hach), a COD reactor (DRM 200, Hach), and an Agilent 9453 UV-visible spectrophotometer. A Carver model C manual press equipped with a digitally temperature-controlled Carver 3796 heated platen set was used to manufacture membrane samples.

10-Bromodeca-1,3-diene. Pyridinium chlorochromate (PCC) on alumina (78.6 g, 91.2 mmol, 178 mol %) was added to a solution of 7-bromo-1-heptanol (10.0 g, 51.3 mmol, 100 mol %) in CH₂Cl₂ (250 mL). The reaction mixture was stirred at room temperature for 16 h, and then the solvent was removed under reduced pressure (35 mm Hg). The brown residue was stirred in diethyl ether (100 mL), filtered through a pad of SiO₂, and washed with diethyl ether (5 x 50 mL). The solvent was removed under reduced pressure (35 mm Hg) to afford 7-bromo-1-heptanal as a light yellow oil (10 g, 97%) that was used without further purification. Matteson's reagent (10.4 g, 43.1 mmol, 120 mol%) was added to a solution of 7-bromo-1-heptanal (6.94 g, 35.9 mmol, 100 mol %) in diethyl ether (125 mL). The reaction was stirred at room temperature for 24 h and then triethanolamine (8.58 g, 57.5 mmol, 160 mol %) was added and the reaction was stirred for an additional 6 h. During this time a white precipitate formed. The reaction mixture was then washed with saturated aq. NaHCO₃ (2 x 100 mL), dried using anhydrous MgSO₄, filtered, and the solvent was removed under reduced pressure (35 mm Hg). The resulting oil was dissolved in diethyl ether (100 mL), H₂SO₄ (0.1 mL) was added, and the reaction was stirred at room temperature for 16 h. The reaction mixture was then poured into a separatory funnel, diluted with diethyl ether (100 mL), and washed with saturated aq. NaHCO₃ (2 x 100 mL). The organic layer was dried (anh. MgSO₄), filtered, and the solvent was removed under reduced pressure (35 mm Hg) to afford the crude product as a light yellow oil. Purification by filtration through a pad of SiO₂ with 6:1 (v/v) hexanes / CH₂Cl₂ (1 L) gave the product as a clear, colorless oil (5.0 g, 66%). ¹H NMR (400 MHz, CDCl₃): δ 6.34 (ddd, *J* = 17.0, 10.4, 10.1 Hz, 1H), 6.09 (dd, *J* = 15.2, 10.4 Hz, 1H), 5.72 (dt, *J* = 15.2, 7.0 Hz, 1H), 5.11 (d, *J* = 17.0 Hz, 1H), 4.94 (d, *J* = 10.1 Hz, 1H), 3.42 (t, *J* = 6.8 Hz, 2H), 2.12 (m, 2H), 1.83 (m, 2H), 1.41 (m, 6H). ¹³C NMR (400 MHz, CDCl₃): δ 137.66, 135.58, 131.38, 115.52, 35.56, 32.65, 32.26, 28.93, 28.15, 27.82. IR (neat): 3082, 3010, 2937, 2845, 1792, 1642, 1459, 1350, 1301, 1260, 1197, 1003, 951, 899, 729. cm⁻¹.

12-Bromododeca-1,3-diene. Synthesized as described in the literature.² Chemical characterization data for the synthesized monomer were consistent with those reported in the literature.²

14-bBromotetradeca-1,3-diene. Synthesized as described in the literature.² Chemical

characterization data for the synthesized monomer were consistent with those reported in the literature.²

1,3-Bis(deca-7,9-dienyl-*N,N,N',N'*-tetramethylammonium)propane dibromide (2a). *N,N,N',N'*-Tetramethyl-1,3-propanediamine (0.150 g, 1.15 mmol, 100 mol %) and 10-bromodeca-1,3-diene (0.512 g, 2.36 mmol, 210 mol %) were dissolved in toluene (10 mL) and acetonitrile (10 mL) in a 50-mL round-bottom flask equipped with a stir bar and a reflux condenser. The clear, colorless solution was heated with stirring to 82 °C for 15 h. The white precipitate that formed after cooling to 0 °C using an ice water bath was filtered and washed with hexanes (2 x 50 mL), affording a white powder (0.5 g, 85%). ¹H NMR (400 MHz, CDCl₃): δ 6.31 (dt, *J* = 10.4, 6.4 Hz, 2H), 6.05 (dd, *J* = 10.4, 4.4 Hz, 2H), 5.68 (dd, *J* = 14.6, 7.6 Hz, 2H), 5.10 (d, *J* = 16.8 Hz, 2H), 4.98 (d, *J* = 10.8 Hz, 2H), 3.93 (t, *J* = 8.0 Hz, 4H), 3.50 (m, 4H), 3.36 (s, 12H), 2.78 (dt, 2H), 2.08 (m, 4H), 1.77 (m, 8H), 1.39 (m, 8H). ¹³C NMR (100 MHz, DMSO-*d*₆): δ 17.09, 22.19, 26.09, 28.62, 28.87, 32.27, 50.70, 59.88, 63.95, 115.71, 131.48, 135.56, 137.65. IR (thin film, MeOH): 3417, 2926, 2854, 2056, 1649, 1483, 1464, 1003, 949, 897, 588 cm⁻¹. HRMS (ES) calcd. for C₂₇H₅₂BrN₂ (M⁺ M⁺ Br⁻): 483.3308; observed: 483.3303.

1,3-Bis(dodeca-9,11-dienyl-*N,N,N',N'*-tetramethylammonium)propane dibromide (2b). *N,N,N',N'*-Tetramethyl-1,3-propanediamine (0.521 g, 4.00 mmol, 100 mol %) and 12-bromododeca-1,3-diene (2.05 g, 8.37 mmol, 209 mol %) were dissolved in toluene (10 mL) and acetonitrile (10 mL) in a 50-mL round-bottom flask equipped with a stir bar and a reflux condenser. The clear, colorless solution was heated with stirring to 82 °C for 15 h. The white precipitate that formed after cooling to 0 °C using an ice water bath was filtered and washed with hexanes (2 x 50 mL), affording a white powder (2.0 g, 89%). ¹H NMR (300 MHz, CDCl₃): δ 6.32 (dt, *J* = 10.3, 17.1, 2H), 6.05 (dd, 2H), 5.71 (dd, 2H), 5.10 (d, 2H), 4.96 (d, 2H), 3.96 (t, 4H), 3.57 – 3.42 (m, 4H), 3.35 (s, 12H), 2.81 (dt, 2H), 2.07 (t, 4H), 1.82 (m, 4H), 1.68 (m, 8H), 1.34 (m, 12H). ¹³C NMR (400MHz, CDCl₃): δ 137.332, 135.398, 130.999, 114.798, 66.501, 60.983, 51.267, 32.521, 29.305, 29.218, 29.112, 29.047, 26.332, 22.979, 18.986. IR (thin film, MeOH): 3437, 2933, 2856, 2094, 1801, 1604, 1651, 1487, 1470, 1003, 951, 899, 723, 650 cm⁻¹. HRMS (ES) calcd. for C₃₁H₆₀BrN₂ (M⁺ M⁺ Br⁻): 539.3934; observed: 539.3913.

1,3-Bis(tetradeca-11,13-dienyl-*N,N,N',N'*-tetramethylammonium)propane dibromide (2c). *N,N,N',N'*-tetramethyl-1,3-propanediamine (1.62 g, 12.4 mmol, 100 mol %) and 14-bromotetradeca-1,3-diene (7.16 g, 26.2 mmol, 211 mol%) were dissolved in toluene (10 mL) and acetonitrile (10 mL) in a 50-mL round-bottom flask equipped with a stir bar and a reflux condenser. The clear, colorless solution was heated with stirring to 82 °C for 15 h. The white precipitate that formed after cooling to 0 °C using an ice water bath was filtered and washed with hexanes (2 x 50 mL), affording a white powder (7.0 g, 87%). ¹H NMR (300 MHz, CDCl₃): δ 6.32 (dt, *J* = 10.2, 17.2, 2H), 6.03 (dd, 2H), 5.72 (dd, *J* = 7.2, 14.8, 2H), 5.09 (d, *J* = 0.6, 2H), 4.96 (d, 2H), 3.96 (t, 4H), 3.56 – 3.43 (m, 4H), 3.36 (s, 12H), 2.81 (t, 2H), 2.07 (m, 4H), 1.75 (m, 8H), 1.32 (m, 24H). ¹³C NMR (75 MHz, CDCl₃): δ 137.48, 135.67, 131.00, 114.75, 66.88, 61.19, 51.42, 32.67, 29.54, 29.42, 29.36, 29.30, 26.45, 23.11, 19.12. IR (thin film, MeOH): 3437, 2933, 2856, 2094, 1801, 1604, 1651, 1487, 1470, 1003, 951, 899, 723, 650 cm⁻¹. HRMS (ES) calcd. for C₃₅H₆₈BrN₂ (M⁺ M⁺ Br⁻): 595.4560; observed: 595.4547.

1,6-Bis(deca-7,9-dienyl-*N,N,N',N'*-tetramethylammonium)hexane dibromide (2d). *N,N,N',N'*-Tetramethyl-1,6-hexanediamine (0.222 g, 1.29 mmol, 100 mol %) and 10-bromodeca-1,3-diene (0.588 g, 2.71 mmol, 210 mol %) were dissolved in toluene (10 mL) and acetonitrile (10 mL) in a 50-mL round-bottom flask equipped with a stir bar and a reflux condenser. The clear, colorless solution was heated with stirring to 82 °C for 15 h. The white precipitate that formed upon cooling to 0 °C using an ice water bath was filtered and washed with hexanes (2 x 50 mL), affording a white powder (0.7 g, 84%). ¹H NMR (300 MHz, CDCl₃): δ 6.33 (dt, 2H), 6.05 (dd, *J* = 10.4, 14.5, 2H), 5.69 (dd, *J* = 7.3, 14.9, 2H), 5.10 (d, *J* = 16.9, 2H), 4.97 (d, *J* = 10.2, 2H), 3.78 (t, 4H), 3.46 (m, 4H), 3.39 (s, 12 H), 2.25 – 1.93 (m, 8H), 1.67 (m, 8H), 1.39 (m, 12H). ¹³C NMR (75 MHz, CDCl₃): δ 137.35, 135.02, 131.40, 115.11, 64.90, 64.35, 51.20, 32.42, 29.01, 28.89, 26.33, 24.40, 23.00, 21.76. IR (thin film, MeOH): 3012, 2931, 2858, 1934, 1716, 1651, 1474, 1398, 1160, 907 cm⁻¹. HRMS (ES) calcd. for C₃₀H₅₈BrN₂ (M⁺ M⁺ Br⁻): 527.3753; observed: 527.3762.

1,6-Bis(dodeca-9,11-dienyl-*N,N,N',N'*-tetramethylammonium)hexane dibromide (2e). *N,N,N',N'*-Tetramethyl-1,6-hexanediamine (0.467 g, 2.71 mmol, 100 mol %) and 12-bromododeca-1,3-diene (1.40 g, 5.71 mmol, 210 mol %) were dissolved in toluene (10 mL) and acetonitrile (10 mL) in a 50-mL round-bottom flask equipped with a stir bar and a reflux condenser. The clear, colorless solution was heated with stirring to 82 °C for 15 h. The white precipitate that formed upon cooling to 0 °C using an ice water bath was filtered and washed with hexanes (2 x 50 mL), affording a white powder (2.0 g, 86%). ¹H NMR (400 MHz, CDCl₃): δ 6.31 (dt, 2H), 6.05 (dd, 2H), 5.70 (dd, 2H), 5.09 (d, 2H), 4.95 (d, 2H), 3.75 (m, 4H), 3.45 (m, 4H), 3.38 (s, 12H), 2.07 (m, 8H), 1.67 (m, 8H), 1.33 (m, 20H). ¹³C NMR (400 MHz, CDCl₃): δ 137.386, 135.509, 131.011, 114.795, 64.738, 64.177, 51.086, 32.556, 29.310, 29.283, 29.139, 29.067, 26.367, 24.565, 22.950, 21.755. IR (thin film, MeOH): 3012, 2927, 2858, 2072, 1716, 1655, 1486, 1471, 1156, 1007, 903, 727 cm⁻¹. HRMS (ES) calcd. for C₃₁H₆₀BrN₂ (M⁺ M⁺ Br⁻): 581.4405; observed: 581.4404.

1,6-Bis(tetradeca-11,13-dienyl-*N,N,N',N'*-tetramethylammonium)hexane dibromide (2f). *N,N,N',N'*-Tetramethyl-1,6-hexanediamine (0.401 g, 2.32 mmol, 100 mol %) and 14-bromotetradeca-1,3-diene (1.29 g, 4.72 mmol, 203 mol%) were dissolved in toluene (10 mL) and acetonitrile (10 mL) in a 50-mL round-bottom flask equipped with a stir bar and a reflux condenser. The clear, colorless solution was heated with stirring to 82 °C for 15 h. The white precipitate that formed upon cooling to 0 °C using an ice water bath was filtered and washed with hexanes (2 x 50 mL), affording a white powder (1.0 g, 83%). ¹H NMR (300 MHz, CDCl₃): δ 6.31 (dt, *J* = 10.2, 16.9, 2H), 6.04 (dd, *J* = 10.3, 15.2, 2H), 5.71 (dd, 2H), 5.08 (d, *J* = 16.9, 2H), 4.95 (d, *J* = 10.2, 2H), 3.75 (m, 4H), 3.46 (m, 4H), 3.39 (s, 12H), 2.06 (m, 8H), 1.66 (m, 8H), 1.31 (m, 28H). ¹³C NMR (75 MHz, CDCl₃): δ 137.53, 135.75, 131.02, 114.77, 77.62, 77.20, 76.78, 65.06, 64.37, 51.23, 32.71, 29.56, 29.55, 29.52, 29.41, 29.33, 26.48, 24.21, 23.05, 21.67. IR (thin film, MeOH): 3008, 2923, 2854, 1651, 1601, 1490, 1471, 1064, 1026, 957, 907, 727 cm⁻¹. HRMS (ES) calcd. for C₃₁H₆₀BrN₂ (M⁺ M⁺ Br⁻): 637.5010; observed: 637.5030.

Determination of LLC phase behavior and LLC phase diagrams. Previously published methods were used to examine the LLC phase behavior.^{3,4} LLC samples of specific composition were made by adding an appropriate amount of monomer, water, and 2-hydroxy-2-

methylpropiophenone (HMP), a photo-initiator (PI), to custom made glass vials, and sealed with Teflon tape and Parafilm. LLC samples were mixed by alternately hand-mixing and centrifuging (3500 rpm) until completely homogenous. It should be noted that the LLC samples are sensitive to evaporative water loss. Special attention was taken to keep the samples sealed as much as possible during sample mixing and transferring to minimize water loss.

The range of each LLC phase was determined using variable-temperature PLM. Specimens were prepared by pressing samples between a microscope slide and microscope cover-slip. The assembly was then placed on the PLM thermal stage and annealed past its isotropic temperature or up to 85 °C (whichever came first). The sample was slowly cooled and allowed to come back to its room temperature phase. The sample was then heated to 95 °C at a rate of 5 °C/min with digital image capture every 1.25 °C and continuous recording of the light intensity. Images were captured at 125x magnification. Changes in optical texture and light intensity were used to determine changes in the LLC phase of the mixture.

The identity of each observed phase was then confirmed by XRD by analyzing a point in each distinct phase region as elucidated by PLM. XRD spectra of the samples were taken either by using a film holder apparatus for room temperature spectra or a heated stage for higher temperature spectra. In the film holder, a sample was placed between Mylar sheets with an appropriate spacer, annealed, placed in the film holder, and then examined. On the heated stage, a sample was placed in an aluminum XRD pan and a piece of Mylar was used to cover the sample to prevent evaporation. The spacing of the XRD peaks is used to determine the LLC phase. Using the combined PLM and XRD data, phase diagrams were plotted for each LLC monomer as a function of composition and temperature.

Phase diagrams of the LLC behavior for gemini ammonium monomers **2a**, **2b**, **2d**, and **2e** are shown in Figure S1. The LLC phase behavior of the monomers **2c** and **2f** are shown in the main body of the manuscript (Figure 3). Compositions, temperatures, and powder XRD data for representative LLC samples are tabulated in Table S1. Representative PLM images of each phase are shown in Figures S2–S5.

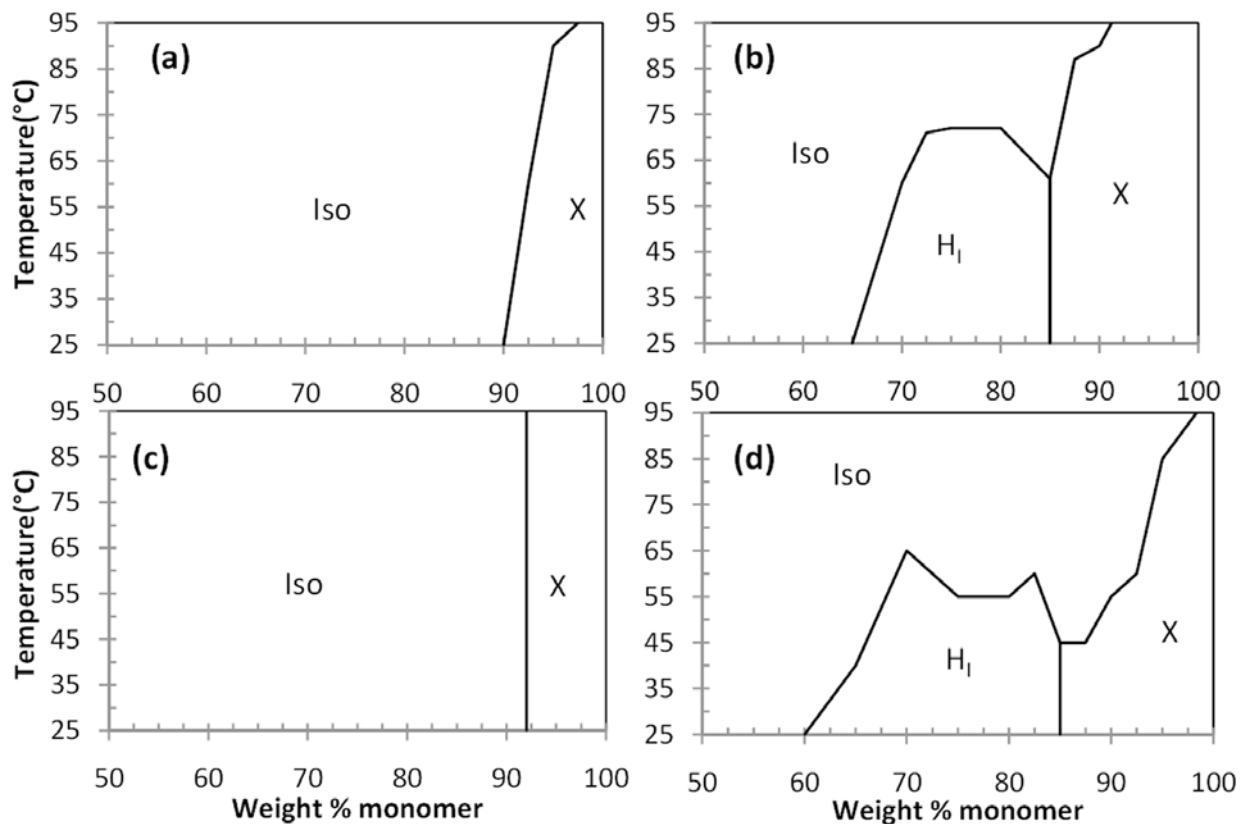


Figure S1. Phase diagrams of (a) monomer **2a** ($x = 6$, $y = 3$), (b) monomer **2b** ($x = 8$, $y = 3$), (c) monomer **2d** ($x = 6$, $y = 6$), and (d) monomer **2e** ($x = 8$, $y = 6$) with water. Iso = an isotropic or pseudo-isotropic phase (e.g., micelles, a discontinuous cubic phase, or a non-ordered phase); H₁ = normal hexagonal phase; Q₁ = normal bicontinuous cubic phase; X = crystalline phase.

Table S1. Compositions, temperatures, and powder XRD peak data for unpolymerized and polymerized gemini ammonium monomer LLC mixtures with water. The temperature refers to the approximate temperature of the LLC mixture during XRD for unpolymerized samples. For polymerized samples (denoted by “polymer” next to the compound label), the temperature refers to the temperature of the sample during polymerization. XRDs were taken at R.T. for polymerized samples. The LLC phases listed were determined by XRD pattern and PLM texture analysis.

Compound	x	y	Composition (wt % monomer)	Temp. (°C)	Powder XRD <i>d</i> -spacing (Å)		LLC phase
2b	8	3	70	R.T.	33.6	19.6	H _I
2b – cross-linked	8	3	70	R.T.	29.8		H _I
2c	10	3	75	40	36.9		H _I
2c – cross-linked	10	3	75	40	31.9	18.6	H _I
2c	10	3	85	60	34.2	27.1	Q _I
2c – cross-linked	10	3	85	60	30.4	27.1	Q _I
2c	10	3	90	80	31.0		L
2c – cross-linked	10	3	90	80	31.3	15.5	L
2e	8	6	70	R.T.	31.6		H _I
2e – cross-linked	8	6	70	R.T.	31.6		H _I
2e	8	6	80	R.T.	29.9		H _I
2e – cross-linked	8	6	80	R.T.	30.1	18.1	H _I
2f – cross-linked	10	6	75	60	30.8	18.2	H _I
2f	10	6	85	60	33.8	28.4	Q _I
2f – cross-linked	10	6	85	60	31.5	27.1	Q _I
2f	10	6	90	90	30.0		L
2f – cross-linked	10	6	90	90	31.7	16.1	L

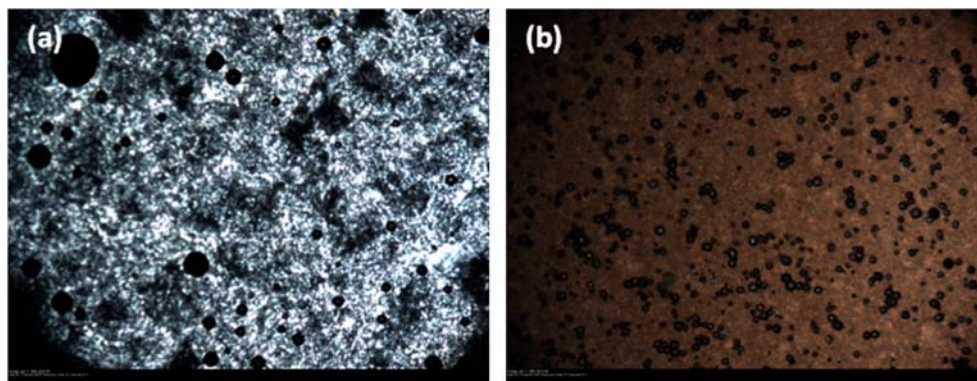


Figure S2. Representative PLM optical textures of LLC mixtures of **2b** (x = 8, y = 3): (a) a H_I phase consisting of 75/25 (w/w) **2b** / water at 30 °C, (b) a crystalline phase consisting of 85/15 (w/w) **2b** / water at 30 °C.

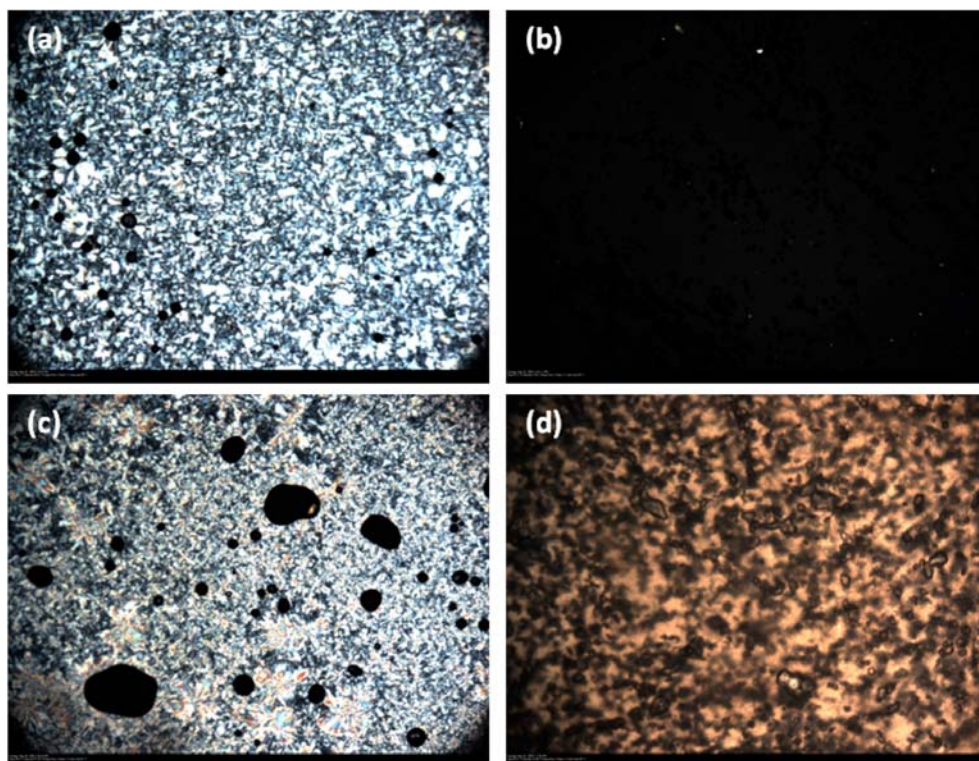


Figure S3. Representative PLM optical textures of LLC mixtures of **2c** ($x = 10, y = 3$): (a) a H_I phase consisting of 65/35 (w/w) **2c** / water at 60 °C, (b) a Q_I phase consisting of 85/15 (w/w) **2c** / water at 60 °C, (c) a L phase consisting of 90/10 (w/w) **2c** / water at 60 °C, and (d) a crystalline phase consisting of 95/5 (w/w) **2c** / water at 60 °C.

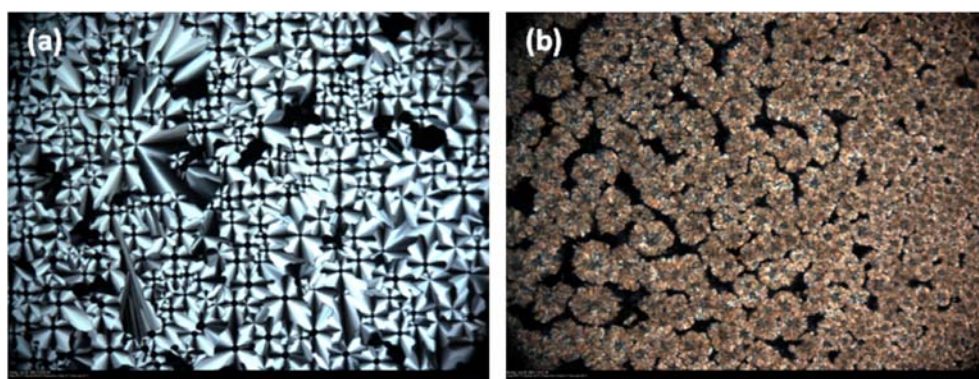


Figure S4. Representative PLM optical textures of LLC mixtures of **2e** ($x = 8, y = 6$): (a) a H_I phase consisting of 72.5/27.5 (w/w) **2e** / water at 50 °C, and (b) a crystalline phase consisting of 90/10 (w/w) **2e** / water at 50 °C.

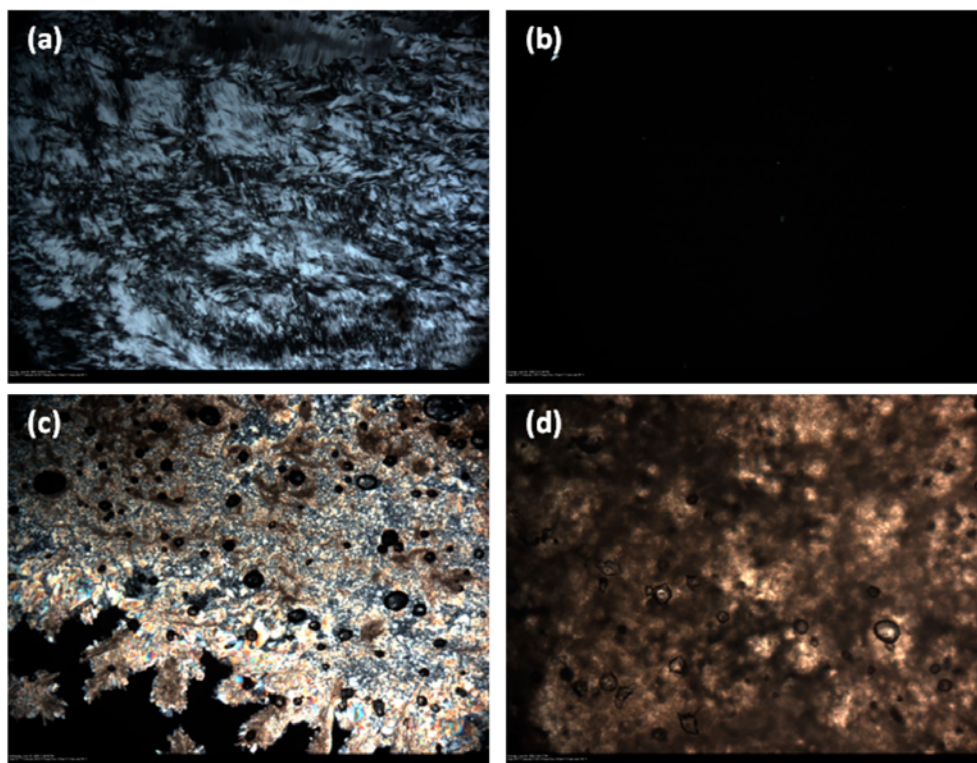


Figure S5. Representative PLM optical textures of LLC mixtures of **2f** ($x = 10$, $y = 6$): (a) a H_I phase consisting of 75/25 (w/w) **2f** / water at 60 °C, (b) a Q_I phase consisting of 85/15 (w/w) **2f** /water at 60 °C, (c) a mixed crystalline/LLC phase consisting of 90/10 (w/w) **2f** / water at 60 °C, and (d) a crystalline phase consisting of 95/5 (w/w) **2f** / water at 60 °C.

Determination of the degree of diene polymerization of bicontinuous cubic (Q_I) phases. LLC samples of 84.2/14.8/1.0 (w/w/w) **2c**/H₂O/HMP and **2f**/H₂O/HMP were made. This specific composition forms a Q_I phase when heated above 50 °C and 55 °C, respectively. Samples were prepared for FT-IR analysis by placing a small amount of LLC sample between two Ge plates with an appropriate spacer and heated to 60 °C to form a Q_I phase. The mixtures between the two Ge plates were then examined using a FT-IR spectrometer to obtain pre-polymerization spectra of the mixtures. Using the same LLC mixtures, a small amount was placed between a Ge crystal plate and quartz plate with the same spacer. The quartz plate minimizes the loss of water in the LLC sample while being transparent to UV light for photopolymerization. Samples were then heated and held at 60 °C to form the Q_I phase and then irradiated with 365 nm light (8.5 mW cm⁻²) for 1 h. The quartz plate was then carefully removed leaving the polymerized LLC sample on the Ge plate. The polymerized sample was then examined using a FT-IR spectrometer to obtain post-polymerization spectra of the mixtures. The 1004 cm⁻¹ absorbance peak in the pre-polymerized samples comes from the C–H out of plane wagging from the –CH=CH₂ located at the end of the diene terminated tails of the monomer.^{3,4} The disappearance of the 1004 cm⁻¹ in the post-polymerized samples suggest >95% degree of 1,3-diene conversion for the Q_I -phase LLC sample.^{3,4} This is more than sufficient to create a highly cross-linked polymer network. Subsequently, PLM and XRD analysis of the polymerized samples showed that it still retained the Q_I -phase nanostructure. The resulting Q_I -phase material

is highly stabilized due to the high degree of cross-linking. The FT-IR spectra showing the pre-polymerized and post-polymerized samples of the two Q_I phases are shown in Figures S6 and S7.

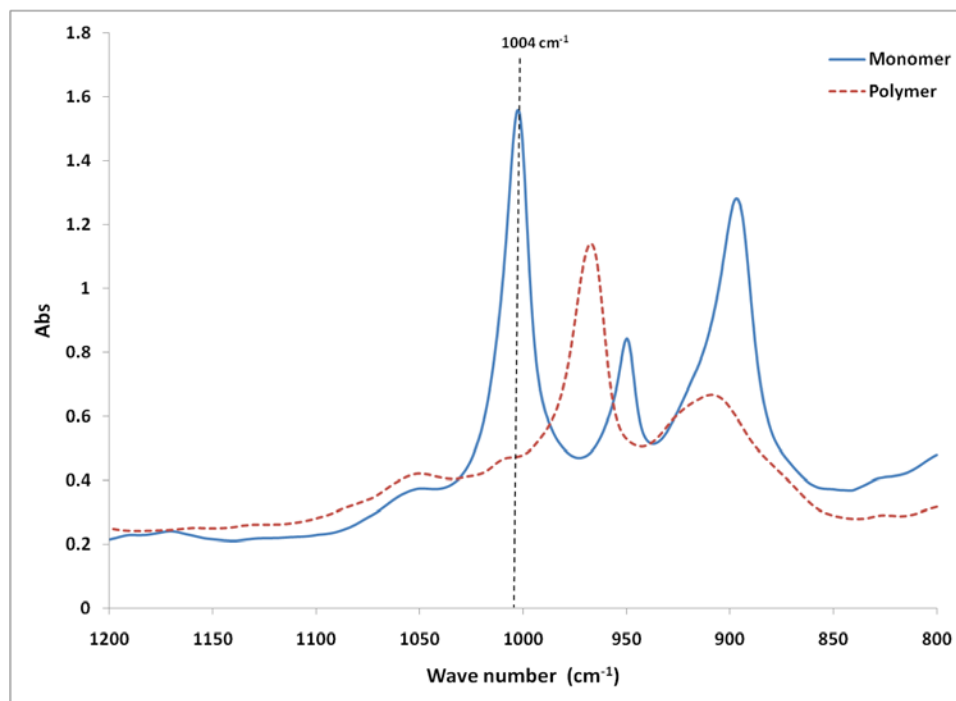


Figure S6. FT-IR spectra of 84.2/14.8/1.0 (w/w/w) **2c**/H₂O/HMP heated to 60 °C before polymerization (monomer mixture) and after 1 h of 365 nm UV light exposure (8.5 mW cm^{-2}) at 60 °C (cross-linked polymer). Disappearance of the 1004 cm^{-1} FT-IR band suggests >95% conversion of the 1,3-diene functional group while in the Q_I phase.^{3,4}

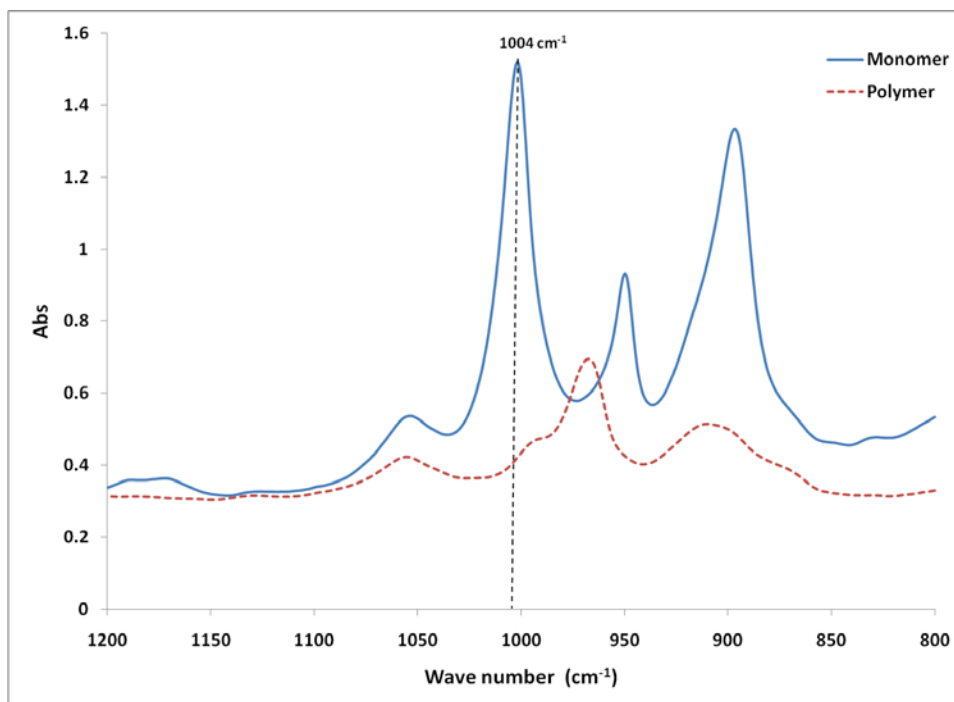


Figure S7. FT-IR spectra of 84.2/14.8/1.0 (w/w/w) **2f**/H₂O/HMP heated to 60 °C before polymerization (monomer mixture) and after 1 h of 365 nm UV light exposure (8.5 mW cm⁻²) at 75 °C (cross-linked polymer). Disappearance of the 1004 cm⁻¹ FT-IR band suggests >95% conversion of the 1,3diene functional group while in the Q_I phase.^{3,4}

Fabrication of supported Q_I-phase membranes of **2c.** Supported membranes of the cross-linked Q_I-phase of monomer **2c** were made using a modified hot-pressing method previously published.⁴ In this process, a Q_I-phase monomer gel mixture containing 84.2/14.8/1.0 (w/w/w) **2c**/H₂O/HMP was prepared. A small amount of the LLC monomer mixture (50–100 mg) was then placed on a piece of Solupor E075-9H01A support membrane. This was then placed between two Mylar sheets to prevent water evaporation. The membrane sample between Mylar sheets was then placed between two mirror-like, polished aluminum plates. The aluminum plates provide a smooth, heat conductive surface for hot-pressing of the membrane assembly. The membrane assembly was then pressed using a Carver manual press equipped with temperature controlled heated platens pre-heated to 60 °C. An applied force of 1–8 tons for 10 min was used to infuse the Q_I-phase monomer mixture completely through the entire depth of the Solupor E075-9H01A support. The membrane sample removed from the press and aluminum plates. It was then clamped between two quartz plates pre-heated to 60 °C and photopolymerized at 60 °C with a 365 nm UV light source (ca. 8.5 mW cm⁻²) for 1 h to radically photo-cross-link the Q_I-phase nanostructure. The quartz plates help minimize water loss during photopolymerization. Cross-linking and stabilization of the Q_I-phase nanostructure in the Solupor E075-9H01A support membrane was verified by powder XRD analysis. Figure S8 shows the Q_I phase was maintained after polymerization in the Solupor E075-9H01A support. The resulting supported membrane appears optically transparent (Figure S9).

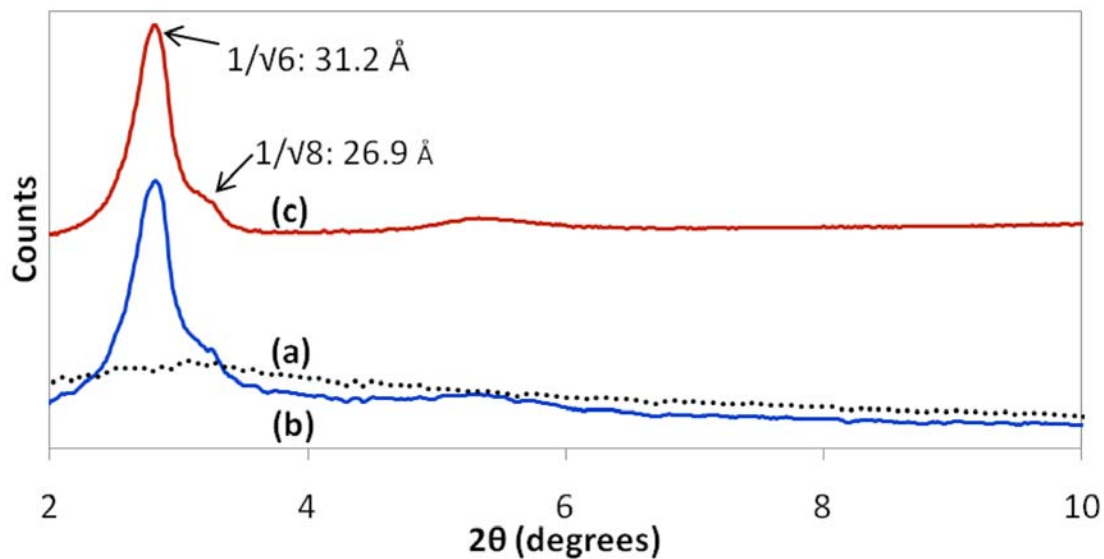


Figure S8. XRD spectra of (a) the Solupor PE support material, (b) the cross-linked Q_I phase of **2c** fully infused in the Solupor PE support material, and (c) the subtraction of the powder XRD profiles of (a) from (b) to give the structure of just the cross-linked Q_I phase of **2c**. The XRD spectrum (c) suggests that the Q_I phase nanostructure is maintained in the polymerized supported membrane.



Figure S9. Picture of a supported cross-linked Q_I-phase membrane of **2c**. Scale: Each grid division is 0.25 of an inch. The polymerized Q_I-phase of **2c** infused into the Solupor support is visually transparent, while the surrounding pristine Solupor support material is not.

Water nanofiltration testing of supported Q₁-phase membranes of 2c. Membrane discs of the supported Q₁-phase membranes of 2c (2.5 cm in diameter) were cut from sheets using a sharpened circular punch die. The membrane discs were installed into custom-made, stainless steel, stirred dead-end filtration cells (Figure S10). The membrane holder has a 2.5 cm outer diameter and an effective filtration area of 3.8 cm². Deionized water was filtered through the membrane using 2.76 x 10⁶ Pa (400 psi) of N₂ pressure as the driving force. The deionized water was filtered at ambient temperature (21 ± 1 °C) until at least 5 mL of permeate was collected. The first filtration with deionized water is to ensure the integrity of the membrane and also to clean out any unpolymerized monomer or other contaminants that might remain in the membrane after processing.

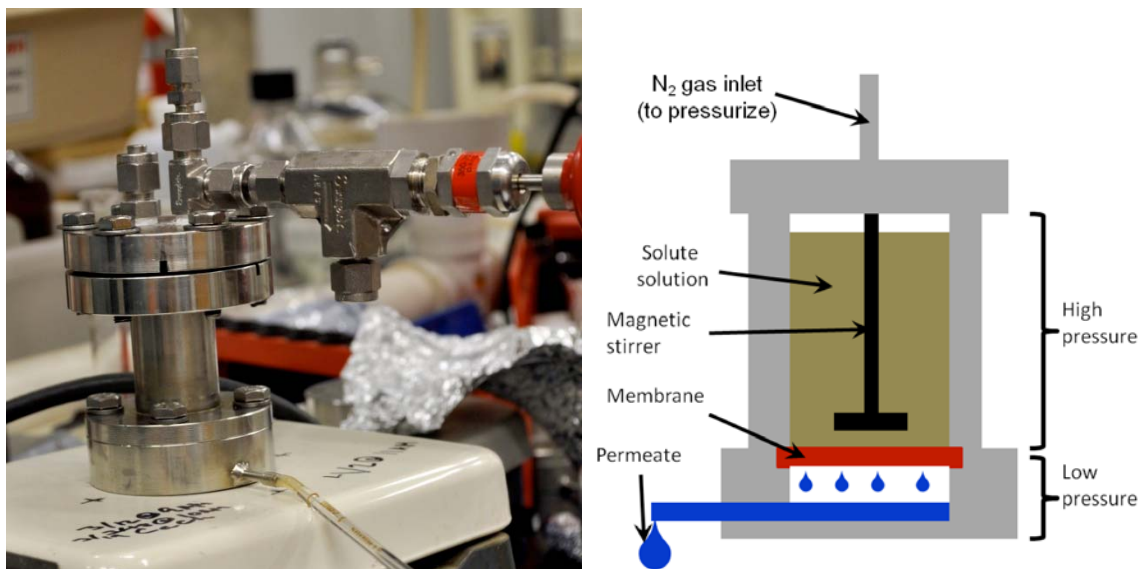


Figure S10. Image and schematic representation of the custom-made, stirred dead-end water filtration cells used in this study.

All filtration experiments were then carried out using aqueous feed solutions containing a single solute at 2000 ppm concentration. Each stirred dead-end filtration cell was loaded with 25 mL of the feed solution and pressurized to 2.76 x 10⁶ Pa (400 psi) of N₂ pressure. The first 1–2 mL of permeate were discarded. The next 2–4 mL of permeate were then collected and examined to determine thickness-normalized permeance and rejection.

For all filtration studies, the thickness-normalized permeance (J) was calculated as follows using Eq. 1:

$$J = \frac{\Delta V}{A \Delta t} \frac{1}{\Delta P} \Delta x, \quad (1)$$

where A is the surface area of the membrane (3.8 cm²), ΔV is the permeate volume, and Δt is the time needed to collect the permeate, ΔP is the transmembrane pressure, and Δx is the membrane thickness. The rejection (R) was calculated as follows using Eq. 2:

$$R = \left(1 - \frac{C_{permeate}}{C_{feed}} \right) \times 100\% , \quad (2)$$

where $C_{permeate}$ and C_{feed} are the concentration of solute in the permeate and feed, respectively. All reported permeances and rejections are averages of three different membrane samples in separated experiments. Reported errors are standard deviations calculated using three different membranes in separate experiments.

Permeate analysis. The concentration of NaCl, KCl, MgCl₂, and CaCl₂ in the permeate solution were determined using an electrical conductivity meter. The conductivity meter was calibrated for each salt using standard aqueous solutions of each salt. The concentrations of all the neutral organic solutions were determined using TOC digestion kit with a modified procedure based on Hach method 10173 and subsequent UV-visible analysis. Calibration plots made with standard solutions prior to each study to ensure accuracy.

Estimation of the effective pore size using the Ferry equation. The Ferry equation (eqn. 3) describes rejection as a function of effective solute size and effective pore size.⁵ This simple steric pore model assumes that the solutes are spherical and the membrane pores are uniform cylinders. The Ferry equation has been used to describe a variety of porous membranes.⁴⁻⁷ The Ferry equation is shown as follows in Eq. 3:

$$R = \left[1 - \left(1 - r_{solute} / r_{pore} \right)^2 \right]^2 \times 100\% , \quad (3)$$

where R is the rejection in percent, r_{solute} is the solute diameter, and r_{pore} is the pore diameter. The observed rejection data of the Q₁-membrane of **2c** for the non-charged solutes (i.e., sucrose, glucose, glycerol, and ethylene glycol) were fitted to the Ferry equation to estimate the effective pore size in the absence of charge-charge effects. The solute diameters used in this study are the same as the values used in a previous study with **1**.⁴ After fitting the rejection data to the Ferry model, it was determined that the effective pore size of the supported Q₁-phase membranes of **2c** is ca. 0.86 nm. This is slightly larger than the ca. 0.75 nm pores found in the 1st-generation Q₁-phase membranes of **1**.⁴ Figure S11 shows that the Ferry equation with a uniform pore size of 0.86 nm is in good agreement with the observed rejection data for the neutral solutes.

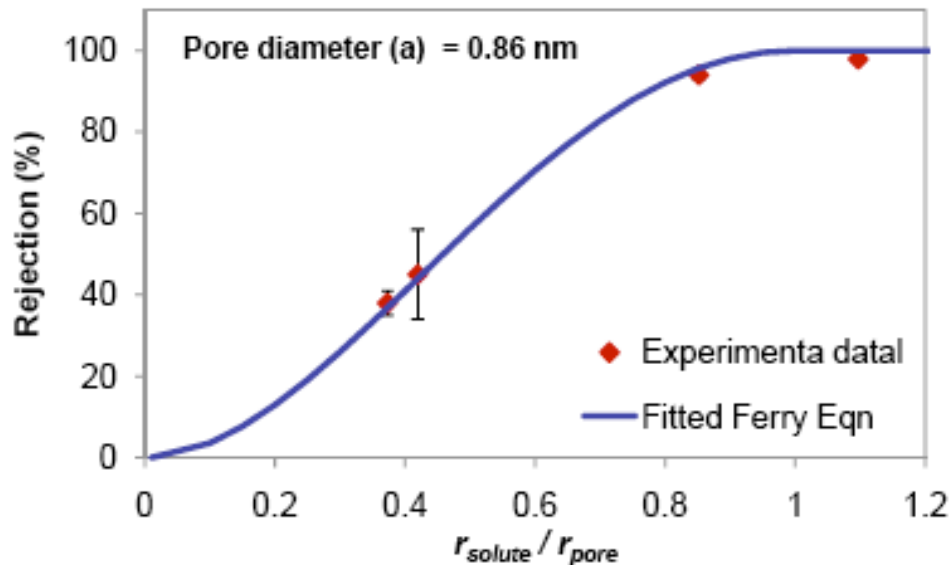
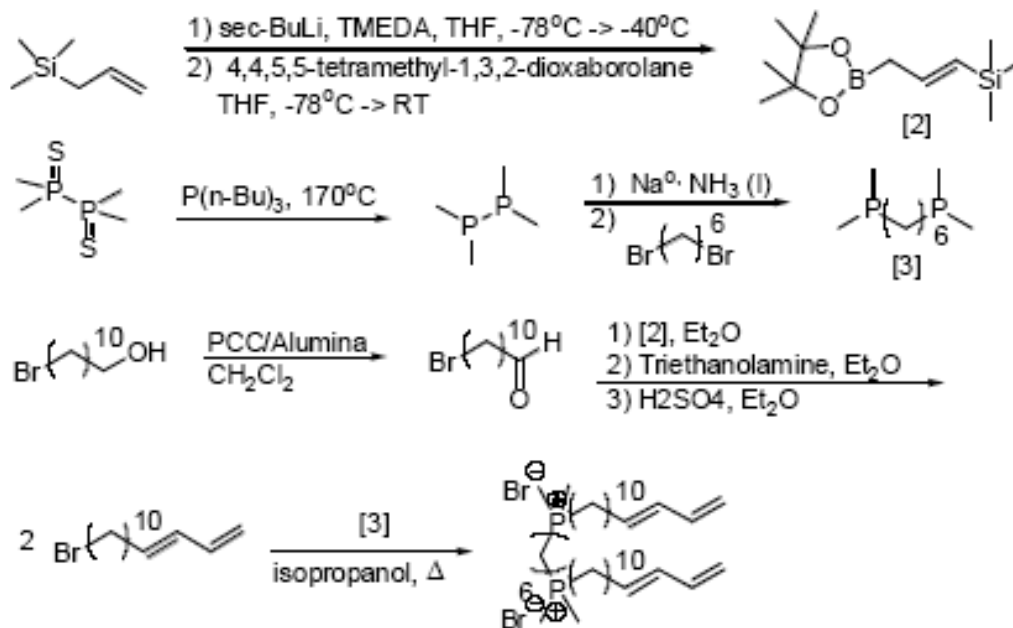
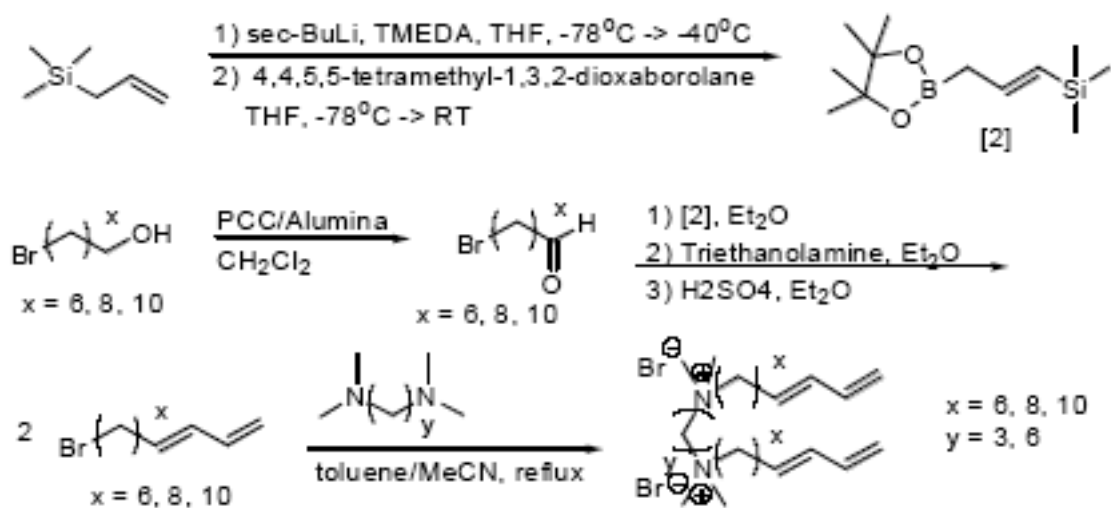


Figure S11. Calculated (Ferry Equation with $r_{pore} = 0.86$ nm) and experimentally measured rejections for the neutral solute molecules. Water filtrations were performed in stirred, dead-end filtration cells with a differential pressure of 2.76×10^6 Pa (400 psi) and a solute concentration of 2000 ppm.

Reagent cost analysis of **2c vs. the gemini phosphonium monomer (**1**).** The cost analysis of the reagents needed to make **2c** and the previously published gemini phosphonium LLC material⁴ are shown in Tables S2–S4. The synthesis schemes are shown in Scheme S1 and S2. Only the reagent costs purchased on the laboratory scale are considered, with observed laboratory scale yields for each reaction. No solvent, purification materials, energy, or time considerations are calculated in these cost estimates for LLC monomer synthesis. Table S2 describes the cost of the intermediate 14-bromotetradeca-1,3-diene. It is an intermediate used in both final products. Table S3 and S4 show that the overall cost of **2c** is much lower than the original gemini phosphonium LLC monomer **1**. The reagents cost of **2c** is approximately \$14.38/g while that of the original gemini phosphonium LLC monomer **1** is \$78.45/g.



Scheme S1: Synthesis scheme for gemini phosphonium LLC monomer.⁴



Scheme S2: General synthesis scheme for homologues of new gemini ammonium LLC monomer 2.

Table S2. Reagent costs for synthesizing the 14-bromotetradeca-1,3-diene tail. It is subsequently used in the synthesis of **2c**, and the previously published gemini phosphonium LLC monomer. The costs listed do not consider solvent, purification materials, energy, or labor.

Compound	Mass	Cost	\$/g	Scale of Reaction	Cost in reaction	Overall \$/g
Chromium (IV) oxide	500 g	\$174.00	\$0.35	30 g	\$10.50	
Brockman Basic Alumina	5 kg	\$287.00	\$0.06	250 g	\$15.00	
Pyridine	982 g	\$141.50	\$0.14	23.8 g	\$3.33	
\$/gram for PCC synthesis				369.75 g	\$28.83	\$0.08
11-bromo-1-undecanol	50 g	\$155.00	\$3.10	16g	\$49.60	
PCC			\$0.08	83 g	\$6.64	
\$/gram for PCC oxidation of aldehyde				14.3 g	\$56.24	\$3.93
<i>N,N,N',N'</i> -tetramethylethylenediamine	77.5 g	\$106.00	\$1.37	18.6 g	\$25.48	
sec-Butyl lithium, 1.4 M in cyclohexane	71.7 g	\$144.80	\$2.02	10.2 g	\$20.60	
Allytrimethylsilane	50g	\$91.60	\$1.83	18.3 g	\$33.49	
2-Isopropoxy-4,4,5,5-tetramethyl-1,3,2-dioxaborolane	91.2g	\$145	\$1.59	27.0 g	\$42.93	
\$/gram for synthesis of Matteson's Reagent [2]				27.7 g	\$122.50	\$4.42
11-bromo-1-undecanal			\$3.93	22.5 g	\$88.43	
Matteson's Reagent			\$4.42	26.8 g	\$118.46	
Triethanolamine	1124 g	\$84.30	\$0.08	21.6 g	\$1.73	
\$/gram of 14-bromotetradeca-1,3-diene				16.3 g	\$208.62	\$12.80

Table S3. Reagent cost of synthesizing the final product **2c**. The listed costs do not include solvent, purification materials, energy, or labor.

Compound	Mass	Cost	\$/g	Scale of Reaction	Cost in reaction	Overall \$/g
14-bromotetradeca-1,3-diene			\$12.80	5.39 g	\$68.99	
<i>N,N,N',N'</i> -tetramethylpropanediamine	77.9 g	\$29.40	\$0.38	1.22 g	\$0.46	
\$/gram of 2c				4.83 g	\$69.45	\$14.38

Table S4. Reagent costs of synthesizing the original gemini phosphonium LLC monomer previously used to make nanostructured polymer membranes for water nanofiltration.^{3,4} The listed costs do not include solvent, purification materials, energy, or labor.

Compound	Mass	Cost	\$/g	Scale of Reaction	Cost in reaction	Overall \$/g
tetramethyldiphosphine disulfide	5 g	\$123.70	\$24.74	25.0 g	\$618.50	
tributyl phosphine	100 g	\$25.00	\$0.25	58.2 g	\$14.55	
\$/g of tetramethyldiphosphine				14.9 g	\$633.05	\$42.49
tetramethyldiphosphine			\$42.49	14.9 g	\$633.05	
sodium (metal)	100 g	\$48.40	\$0.48	2.85 g	\$1.37	
ammonia (liquid)	170 g	\$435.00	\$2.56	68.2 g	\$174.59	
1,6-dibromohexane	500 g	\$76.50	\$0.15	15.68 g	\$2.35	
\$/g of 1,6-bis(dimethylphosphino)hexane				4.840 g	\$811.36	\$167.63
1,6-bis(dimethylphosphino)hexane			\$167.63	4.840 g	\$811.36	
14-bromotetradeca-1,3-diene			\$12.80	13.47 g	\$172.42	
\$/g of gemini phosphonium (1)				12.54 g	\$983.78	\$78.45

References

- (1) Blanton, T. N.; Huang, T. C.; Toraya, H.; Hubbard, C. R.; Robie, S. B.; Louer, D.; Gobel, H. E.; Will, G.; Gilles, R.; Raftery, T. *Powder Diffr.* **1995**, *10*, 91–95.
- (2) Hoag, B. P.; Gin, D. L. *Macromolecules* **2000**, *33*, 8549–8558.
- (3) Pindzola, B. A.; Jin, J.; Gin, D. L. *J. Am. Chem. Soc.* **2003**, *125*, 2940–2949.
- (4) Zhou, M. J.; Nemade, P. R.; Lu, X. Y.; Zeng, X. H.; Hatakeyama, E. S.; Noble, R. D.; Gin, D. L. *J. Am. Chem. Soc.* **2007**, *129*, 9574–9575.
- (5) Ferry, J. D. *Chem. Rev.* **1936**, *18*, 373–455.
- (6) Gibbins, E.; D' Antonio, M.; Nair, D.; White, L. S.; Freitas dos Santos, L. M.; Vankelecom, I. F. J.; Livingston, A. G. *Desalination* **2002**, *147*, 307–313.
- (7) Geens, J.; Boussu, K.; Vandecasteele, C.; Van der Bruggen, B. *J. Membr. Sci.* **2006**, *281*, 139–148.